Virtual Variable Sampling Discrete Fourier Transform based Selective Odd-order Harmonic Repetitive Control of DC/AC Converters

Zhichao Liu, *Student Member*, *IEEE*, Bin Zhang, *Senior Member*, *IEEE*,
Keliang Zhou, *Senior Member*, *IEEE*, and Jingcheng Wang, *Senior Member*, *IEEE*

***Abstract*—This paper proposes a frequency adaptive discrete Fourier transform (DFT) based repetitive control (RC) scheme for DC/AC converters. By generating infinite magnitude on the interested harmonics, the DFT-based RC offers a selective harmonic scheme to eliminate waveform distortion. The traditional DFT-based selective harmonic RC, however, is sensitive to frequency fluctuation since even very small frequency fluctuation leads to a severe magnitude decrease. To address the problem, virtual variable sampling method, which creates an adjustable virtual delay unit to closely approximate a variable sampling delay, is proposed to enable the DFT-based selective harmonic RC to be frequency adaptive. Moreover, a selective odd-order harmonic DFT filter is developed to deal with the dominant odd order harmonic. Because it halves the number of sampling delays in the DFT filter, the system transient response gets nearly 50% improvement. A comprehensive series of experiments of the proposed VVS DFT-based selective odd-order harmonic RC controlled programmable AC power source under frequency variations are presented to verify the effectiveness of the proposed method.**

***Index Terms*—Repetitive control, DC/AC converter, DFT, frequency fluctuation, selective harmonics, virtual variable sampling.**

I. Introduction

DC/AC pulse-width modulated (PWM) power converters are widely used as a significant element in nowadays power conversion applications, e.g. uninterrupted power supply system, renewable energy source converter, programmable AC power source, and other power electronics applications [1]–[9]. For instance, programmable AC power sources provide adjustable sinusoidal output voltages in various bench-top tests, International Electrotechnical Commission (IEC) tests, and power supply tests. Such power supply systems suffer from various disturbances including modeling uncertainty and frequency fluctuation in practical applications. The control method for such systems must be stable and robust to frequency fluctuation and load uncertainties. Although traditional control methods such as proportional-integral (PI) control and state feedback control can stabilize the system, they often cannot ensure satisfactory control accuracy for periodic reference signal tracking and disturbance rejection.

Repetitive control (RC) is an advanced and effective method for periodic signal tracking, which can improve the converter performance with low total harmonic distortion (THD), fast transient response, and low steady state error [10], [11]. To further improve the stability and selectively eliminate harmonic distortions, the DFT-based selective harmonic RC is proposed [12], [13]. The advantages of the DFT-based selective harmonic RC include: it is a selective harmonic RC scheme, which is more effective to compensate harmonic distortion because major waveform distortion mainly concentrates on low odd harmonics; the DFT-based selective harmonic RC has a narrow bandwidth that enables it to deal with distortion on the interested low order harmonics without affecting overall system stability, such as phase margin and gain margin, while traditional RC requires a low-pass filter to maintain the overall system stability. In the DFT-based selective harmonic RC, a selective harmonic filter is created by using the inverse DFT transformation, where the time-consuming filter coefficient calculation is often done offline. Note that the order of the DFT filter is also the sampling number in one reference signal period, and it should be an integer. It is hard to enable the integer-order DFT filter to deal with varying frequency quasi-periodic signals since it is time-consuming to calculate the filter coefficients for a varying integer-order DFT filter in real time or it is impossible to create a fractional-order DFT filter. Since the traditional DFT-based selective harmonic RC is sensitive to the frequency variation, when the signal frequency deviates from the nominal frequency, the performance of the DFT-based selective harmonic RC degrades severely at the fixed sampling rate.

To address the varying-frequency issue, variable sampling/switching frequency techniques were developed to obtain a fixed integer samples per period for wind and aircraft power systems [14], [15]. However, variable sampling methods not only require special variable sampling processing capabilities of the system CPU, but also need to recalculate other digital control parameters to maintain the system stability and robustness [16], [17]. A parallel structure fractional RC scheme was developed [18] in which a correction factor in complex number is inserted to adjust the poles for each parallel RC controller. One major limitation of this approach is that it is difficult to implement the complex correction

Z. Liu, B. Zhang are with the Department of Electrical Engineering, University of South Carolina, Columbia, SC 29205 USA (e-mail: zhichao@email.sc.edu; zhangbin@cec.sc.edu)

K. Zhou is with the School of Engineering, University of Glasgow, Glasgow G12 8QQ, UK (e-mail: keliang.zhou@glasgow.ac.uk).

J. Wang is with the Department of Automation, Shanghai Jiaotong University, Shanghai 200240 China (e-mail:jcwang@sjtu.edu.cn.)

factor in most digital controllers. Non-integer delay length approximated by a finite impulse response (FIR) filter [19]–[24] and linear-phase-lag low-pass filter for fractional delay length compensation [25] were also developed. However, these frequency adaptive methods cannot be applied to the DFT-based selective harmonic RC.

This paper develops a virtual variable sampling (VVS) method to enable the DFT-based selective harmonic RC at a fixed sampling frequency to achieve an accurate, efficient, and robust RC scheme under frequency fluctuation, where the virtual variable sampling delay is well approximated by a VVS unit. Similar to the variable sampling methods by hardware [14], [15], all the offline-calculated coefficients for the DFT filter can keep invariant during the system operation. When frequency varies or fluctuates, the resonant frequency of the DFT-based selective harmonic RC can be adjusted accordingly by changing the coefficients of VVS. Since only several particular odd-order harmonics usually dominate the distortion in practical applications, it is effective to have a selective odd-order harmonic RC to exclusively deal with the signal at the interest harmonic frequencies [26], [27]. Consequently, a VVS DFT-based selective odd-order harmonic RC scheme is developed. Comparing with traditional DFT-based selective harmonic RC, the proposed RC scheme has an only half number of sampling delay which results in half delay time, so it leads to fast transient response.

The remainder of this paper is organized as follows: Section II introduces the traditional RC, the DFT-based selective harmonic RC, and the virtual variable sampling method. The experimental verification of programmable AC power source with adjustable frequency is presented in Section III, which is followed by the conclusions in Section IV.

II. Virtual Variable Sampling DFT-based Selective Odd-order Harmonic RC

A. Repetitive control

Fig. 1 shows a typical digital control system with plug-in RC controller [10], where $R(z)$ is the periodic reference input with reference frequency f_r and reference period $T_r = 1/f_r$, $G_c(z)$ is the conventional feedback controller, $G_p(z)$ is the plant model, $D(z)$ is the disturbance, $Y(z)$ is the system output, and system sampling frequency is f_s. Plug-in RC controller is a feedforward controller that consists of RC gain K_r, robustness filter $Q(z)$, phase lead filter $G_f(z)$, and period delay z^{-N} in which integral delay length $N = \lfloor T_r/T_s \rceil$ is the nearest integer to the ratio of reference period T_r to the sampling period $T_s = 1/f_s$.

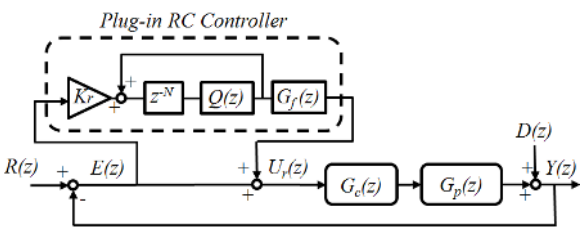

Fig. 1. Control system with plug-in RC controller

The transfer function of the conventional RC $G_{rc}(z)$ in Fig. 1 is:

$$G_{rc}(z) = \frac{U_r(z)}{E(z)} = K_r \frac{z^{-N}Q(z)}{1 - z^{-N}Q(z)} G_f(z) \tag{1}$$

where $E(z) = R(z) - Y(z)$ is the system tracking error. The overall system holds the two stability conditions [11], [22]: the closed-loop feedback system without RC is stable, and

$$|Q(z)(1 - K_r G_f(z) G(z))| \leq 1 \tag{2}$$

where $G(z)$ is the closed-loop transfer function without plug-in RC, $G(z) = G_c(z)G_s(z)/(1 + G_c(z)G_s(z))$. In the frequency domain, RC transfer function in Eq. (1) produces infinite magnitude gain at all harmonic frequencies of the reference signal when $Q(z) = 1$. Therefore, RC can achieve zero steady-state error tracking of periodic signals. In practice, a low-pass filter $Q(z)$, with the form of $Q(z) = a_1 z + a_0 + a_1 z^{-1}$ $(2a_1 + a_0 = 1)$, is added to ensure the system stability. Fig. 2 shows the bode plot of the closed-loop system with a state feedback (SF) controller before and after a plug-in RC is added. It is clear that RC generates magnitude peaks at all harmonic frequencies and the peak magnitudes at high order harmonics are attenuated by the filter $Q(z)$ to guarantee the positive phase margin and gain margin.

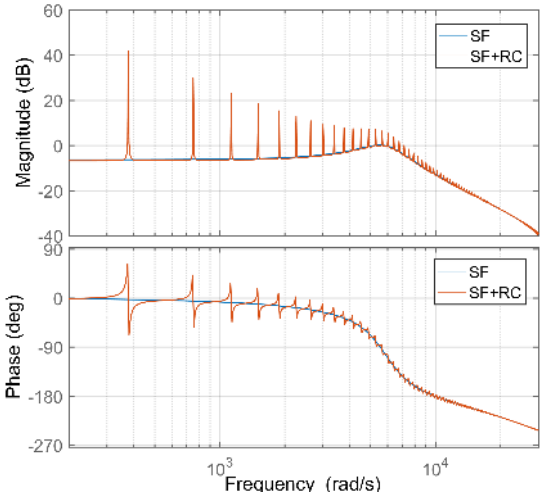

Fig. 2. Bode plot for state feedback (SF) and repetitive controllers (RC) with low-pass filter $Q(z)$

B. The DFT-based selective odd-order harmonic repetitive control

As odd-order harmonics usually dominate the waveform distortion in practice, a DFT-based selective harmonic RC is added as a feedforward controller to boost loop gains at selected odd-order harmonic frequencies [12], [13]. Fig. 3 shows the scheme of the DFT-based selective harmonic RC, in which K_r is RC gain, N_a is phase lead step, and $F_{DFT}(z)$ is a FIR filter in which $b(i)$ is the FIR coefficients. The transfer function of the DFT-based selective harmonic RC is

$$G_{DFT-RC} = K_r \frac{F_{DFT}(z)}{1 - F_{DFT}(z) \cdot z^{-Na}} \tag{3}$$

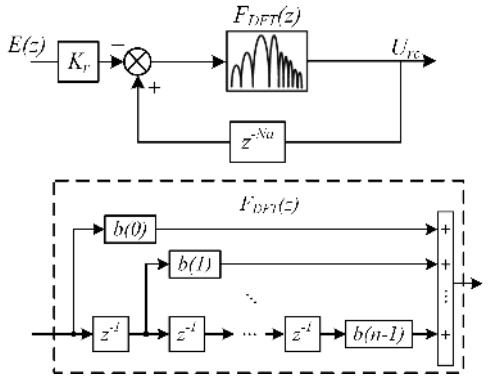

Fig. 3. The DFT-based selective harmonic RC structure

To attain infinite gains at interested dominant odd-order harmonics, $F_{DFT}(z)$ filter is designed with unity gain and zero phase at interested harmonics. Based on inverse discrete Fourier transform, $F_{DFT}(z)$ filter, with a window length equal to half fundamental period of the reference signal T_r, has the transfer function as:

$$F_{DFT}(z) = \frac{4}{N}\sum_{i=0}^{N/2-1}\left(\sum_{h\in N_h} cos\left[\frac{2\pi}{N}h(i+N_a)\right]\right)z^{-i} \quad (4)$$

where N is one fundamental period delay length, i.e. $N = T_r/T_s$, N_h is the set of selected odd-order harmonic frequencies, and N_a is phase lead step that is similar to the one in the traditional RC [11]. The magnitude analysis of $F_{DFT}(z)$ can be found in the proof in Appendix. As an example, for N = 200, N_a = 3, and N_h = 7, the corresponding magnitude response of $F_{DFT}(z)$ is given in Fig. 4 (a), which only allows the 7th order harmonic to pass through with unit magnitude.

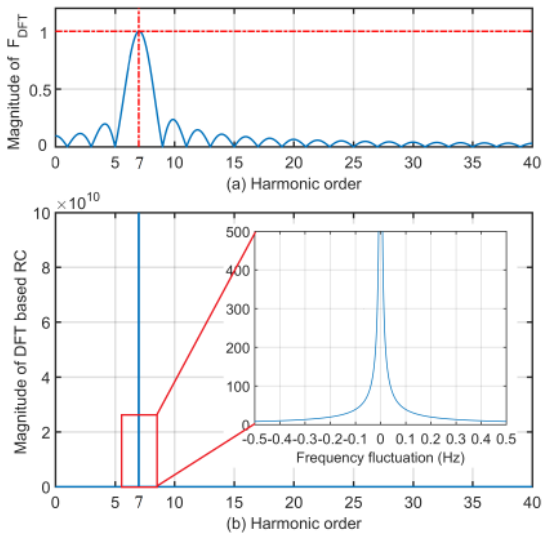

Fig. 4. Magnitude response of $F_{DFT}(z)$ with N=200, N_a=3, and N_h=7

With unity magnitude of $F_{DFT}(z)$ at the selected $7th$ order harmonics frequency, the magnitude of the DFT-based selective harmonic RC in Eq. (3) reaches infinity at the interested $7th$ order harmonics as shown in Fig. 4 (b), thus a selective harmonic RC is achieved. The proposed DFT-based selective odd-order harmonic RC has an only half number (i.e. $N/2$) of delay elements compared with the traditional DFT-based selective harmonic RC with a full number (i.e. N) of delay elements. The merits of the proposed RC scheme is that it achieves faster response since only half delay units are applied in the controller structure. Because the large gain happens only at selected odd-order harmonic frequencies, the proposed RC scheme does not influence the overall system stability characteristics, such as phase margin and gain margin as shown in Fig. 5.

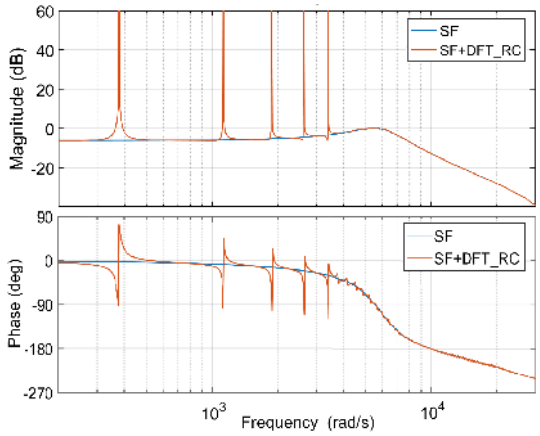

Fig. 5. Bode plot for state feedback and the DFT-based selective harmonic RC on interested harmonics $N_h = 1, 3, 5, 7, 9$

However, the signal frequency fluctuation will severely degrade the performance of the DFT-based selective harmonic RC. The zoomed inset in Fig. 4 (b) shows that when the signal frequency deviates from the nominal frequency, the magnitude of the DFT-based selective harmonic RC decreases significantly: the magnitude drops from infinity to less than 50 when there is only a 0.1 Hz deviation. It is unfeasible to redesign the DFT filter in Eq. (4) by updating the delay number N in each sampling period to achieve real-time control. Therefore, the traditional DFT-based selective harmonic RC is unable to efficiently deal with frequency fluctuation, which exists in most practical systems.

C. Virtual variable sampling DFT-based selective odd-order harmonic repetitive control

To enable the DFT-based selective odd-order harmonic RC to be frequency adaptive, the VVS method is developed in this section. In the proposed RC scheme, all the coefficients of the DFT filter do not need change when the frequency varies or fluctuates. The infinite magnitude gain of RC at the selective order of harmonics is achieved by changing the coefficients of VVS, which is simple, flexible, low-cost, and easy-to-implement.

To develop the proposed VVS, a virtual variable sampling frequency with sampling period T_v is proposed. In this method, the virtual variable sampling period T_v is created to approximate a virtual unit delay to maintain sampling period T_v as an fixed integral multiple N_v of the reference

fundamental period T_r, while the system sampling period T_s keeps a fixed value:

$$T_v = \frac{T_r}{N_v} \tag{5}$$

When T_r changes or fluctuates, T_v can be easily changed by tuning the parameters of VVS to keep N_v as a constant integer. This is equivalent to the solutions with physical varying sampling frequency [14], [15]. The advantage of the proposed approach over previous approaches is that it is more cost efficient than hardware-based methods. It provides a generic solution to frequency adaptive problems and can be used for all delay-based repetitive control design.

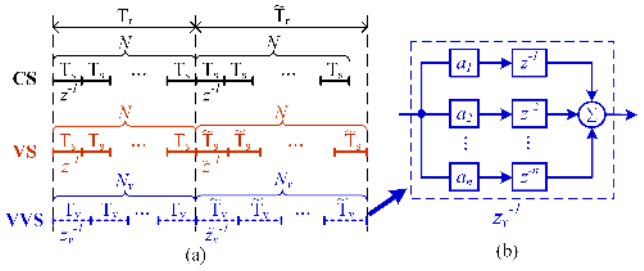

Fig. 6. Sampling points comparison under a sudden reference period change

Fig. 6 (a) shows sampling points comparison under a sudden reference period change between constant sampling (CS), variable sampling (VS), and virtual variable sampling (VVS). When the reference period changes from T_r to $\widetilde{T}_r$, CS cannot provide fixed integer number of delay periods N for both T_r and $\widetilde{T}_r$. By changing sampling period from T_s to $\widetilde{T}_s$ accordingly, VS has integer number N delay periods for both T_r and $\widetilde{T}_r$. With the same sampling period as that in CS, VVS builds approximated virtual variable delay periods T_v and $\widetilde{T}_v$, which is achieved from Fig. 6 (b) with two different sets of parameters, to keep a virtual but fixed number N_v delay periods for both T_r and $\widetilde{T}_r$ without changing system sampling period T_s.

With virtual variable sampling period T_v, the VVS unit delay z_v^{-1} is approximated by establishing a nth-order Lagrange interpolation polynomial:

$$z_v^{-1} = \sum_{i=1}^{n} a_i z^{-i}, \text{with} \quad a_i = \prod_{j=1, j\neq i}^{n} \frac{T_v - iT_s}{jT_s - iT_s} \tag{6}$$

Higher order approximation can provide higher accuracy in approximating a variable sampling unit delay. However, higher order approximation costs more computation and a more complicated design. With the tradeoff of approximation accuracy and design complexity, a 3rd-order polynomial is selected in practical applications. Fig. 7 shows the magnitude response of a 3rd-order VVS unit z_v^{-1} when the reference signal frequency changes from 59 Hz to 61 Hz, where the VVS is designed at 10 kHz sampling frequency. When reference signal frequency deviates away from 60 Hz with $\delta = (f - 60)$ Hz representing the frequency deviation, VVS unit presents an accurate magnitude at 1 when input signal frequency is below 700 Hz for the system with 10 kHz sampling frequency.

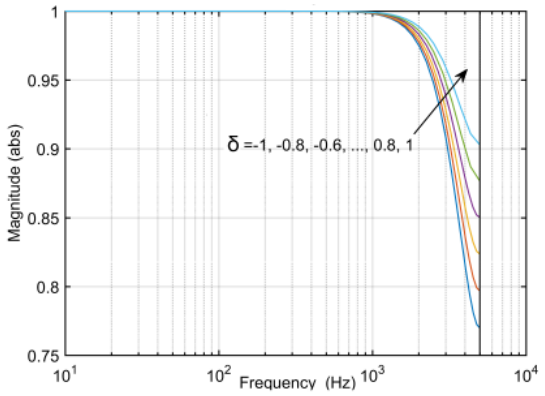

Fig. 7. Magnitude response of VVS unit z_v^{-1}, where $\delta = (f - 60)$ Hz representing the frequency deviation ($f_s = 10$ kHz and $N_v = 80$)

With the VVS unit delay of z_v^{-1} in Eq. (6), the VVS DFT-based selective odd-order harmonic RC has the transfer function as:

$$F_{DFT}(z_v) = \frac{4}{N_v} \sum_{i=0}^{N_v/2-1} \left(\sum_{h \in N_h} cos\left[\frac{2\pi}{N_v} h(i + N_a) \right] \right) z_v^{-i} \tag{7}$$

By applying VVS, the infinite magnitude frequency of the DFT-based selective harmonic RC is able to follow the varying frequency because the virtual sampling frequency can be easily adjusted. Compared with the traditional DFT filter transfer function (4), the delay unit z^{-1} is replaced by the VVS unit z_v^{-1}. Furthermore, the sampling period of input and output still keeps the system sampling period T_s, while all RC analysis in [11] can be conducted with the virtual sampling period T_v. Different from the multi-rate sampling [28], aliasing and imaging do not exist in VVS, which eliminate the design of anti-aliasing and anti-imaging filters.

III. Experimental Verification: Single-Phase Programmable AC Power Supply

A. System Modeling and State Feedback Controller

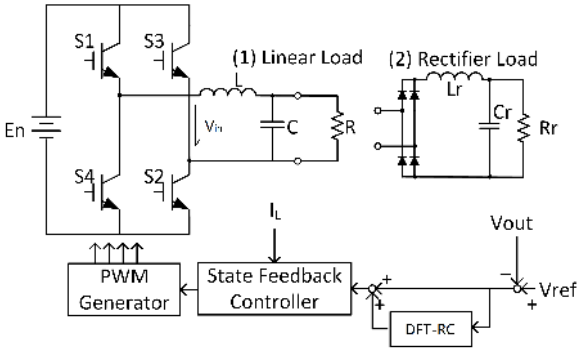

Fig. 8. Plug-in MRC controlled inverter system

Fig. 8 shows a DFT-based selective odd-order harmonic RC controlled single-phase programmable AC power source of DC/AC inverter, where E_n is the DC bus voltage; L and C form an LC filter. The performance of AC source are tested

under linear load R and nonlinear rectifier load with C_r, L_r, and R_r. The output voltage V_{out} and inductor current I_L are two states for state feedback controller; V_{in} is the input PWM voltage.

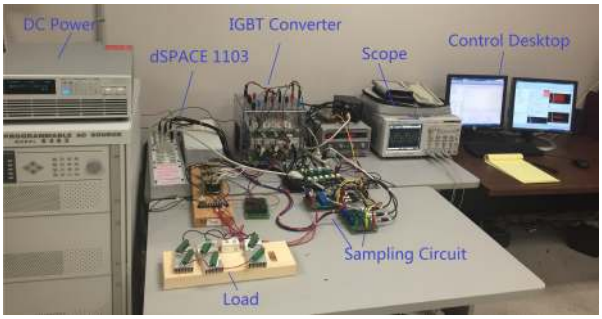

Fig. 9. Experiment setups

Fig. 9 shows the experimental testbed, in which the state feedback controller and plug-in VVS DFT-based selective odd-order harmonic RC are designed in Matlab Simulink and implemented by dSPACE DC1103 to control the H-bridge IGBT converter. The output voltage and current waveform are recorded via sampling circuit by ControlDesk for real-time control and performance analysis.

With the sampling period T_s, the discrete-time state space of the single-phase inverter system in Fig. 8 can be written as:

$$\begin{bmatrix} v(k+1) \\ i(k+1) \end{bmatrix} = \begin{pmatrix} \varphi_{11} & \varphi_{12} \\ \varphi_{21} & \varphi_{22} \end{pmatrix} \begin{bmatrix} v(k) \\ i(k) \end{bmatrix} + \begin{pmatrix} g_1 \\ g_2 \end{pmatrix} u(k) \quad (8)$$

where $\varphi_{11} = 1 - T_s/(RC) + T_s^2/(2R^2C^2) - T_s^2/(2LC)$, $\varphi_{12} = T_s/C - T_s^2/(2RC^2)$, $\varphi_{21} = -T_s/L + T_s^2/(2RLC)$, $\varphi_{22} = 1 - T_s^2/(2LC)$, $g_1 = E_n T_s^2/(2LC)$, $g_2 = E_n T_s/L$ [22].

The state feedback controller has the form as:

$$u = -k_1 v(k) - k_2 i(k) + g v_{ref}(k) \quad (9)$$

where k_1, k_2 and g are state feedback controller parameters, v_{ref} is the reference sinusoidal voltage. With state feedback controller (9), the transfer function can be rewritten as:

$$G(z) = \frac{m_1 z + m_2}{z^2 + p_1 z + p_2} \quad (10)$$

where $p_1 = -(\varphi_{22} - g_2 k_2) - (\varphi_{11} - g_1 k_1)$, $p_2 = (\varphi_{11} - g_1 k_1)(\varphi_{22} - g_2 k_2) - (\varphi_{12} - g_1 k_2)(\varphi_{21} - g_2 k_1)$, $m_1 = g_1 k$, $m_2 = g_2 k - g_1 k(\varphi_{22} - g_2 k_2)$ [11].

TABLE I
SYSTEM PARAMETERS

Parameter	Value	Parameter	Value
DC voltage, E_n	250 V	Inductor, L	3 mH
Capacitor, C	10 μF	PWM frequency	10 kHz
Sampling frequency, f_s	10 kHz	Linear load, R	200 Ω
Rectifier capacitor C_r	60 μF	Rectifier inductor L_r	3 mH
Rectifier resistance R_r	200 Ω		

With parameters in Table I and state feedback controller $k_1 = 0.4$, $k_2 = 7$, and $g = 1.4$, the closed-loop transfer function for 60 Hz single-phase 110V DC/AC inverter is derived as:

$$G(z) = \frac{0.592z + 0.012}{z^2 - 0.81z} \quad (11)$$

The feedback control system is stable with poles $p_1 = 0$, $p_2 = 0.81$ in the unit cycle. With only feedback controller, a severe phase lag and high waveform distortion are observed in the output waveform under linear load and rectifier load conditions shown in Fig. 10. The major distortion components appear on first 10 harmonic frequencies.

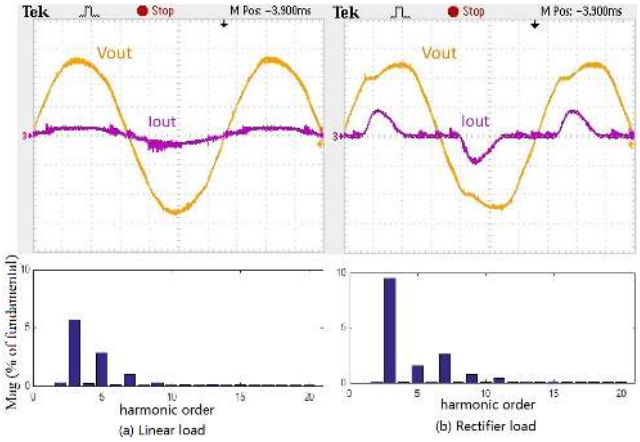

Fig. 10. Experimental result under state feedback control

B. VVS DFT-based selective odd-order harmonic RC design

With the reference signal frequency $f_r = 60$ Hz ($T_r = 1/60$s) and sampling frequency $f_s = 10$ kHz ($T_s = 0.1\mu$s), the delay length for the traditional DFT-based selective harmonic RC is the closest sampling integer $N = \lfloor T_r/T_s \rceil = \lfloor 166.67 \rceil = 167$. From the form of VVS unit delay in Eq. (6), z_v^{-1} is approximated by z^{-1}, z^{-2}, and z^{-3}. The adjustable VVS period is between T_s and $3T_s$, which makes the virtual variable frequency varies between $f_s/3$ and f_s. Delay length N_v in the experiment is selected as 80 where the virtual sampling period is around $2T_s$, thus VVS can have large frequency adjustment range around the reference frequency. The VVS unit delay is obtained from Eq. (6) as:

$$z_v^{-1} = 0.038z^{-1} + 0.993z^{-2} + 0.045z^{-3} \quad (12)$$

Since the distortion appears mainly on $3rd, 5th, 7th$, and $9th$ order harmonics shown in Fig. 10, the selected harmonic set N_h in Eq. (7) is set as $N_h = 1, 3, 5, 7, 9$; The phase lead step N_a is designed to cancel the DSP computational delay and phase delay of plant $G_p(z)$. The design of RC gain K_r and phase lead step N_a can be found in [11], [29], which is based on the accurate system modeling. In practice, the theoretical value does not make the system work at the best state because of system uncertainty and DSP computation delay [30], [31]. By experimental tests,

the RC gain K_r is set as $K_r = 1$ to achieve a fast response to a load or frequency change; the phase lead step N_a is selected as $N_a = 3$, which provides phase lead compensation for model phase lag and computational time delay. The coefficients of the DFT filter $F_{DFT}(z)$ are calculated offline. When reference frequency changes, the VVS unit delay is updated based on Eq. (6).

C. Experimental results and comparison

Programmable AC power sources provide frequency and amplitude adjustable AC voltage for different applications. Under various conditions, a high-performance programmable AC power source is required to generate the very clean sinusoidal output voltage. The system performances are compared between the traditional DFT-based selective harmonic RC and VVS DFT-based selective odd-order harmonic RC in terms of transient response, steady-state performance, load switch, and frequency fluctuation under different kinds of loads at variable frequencies.

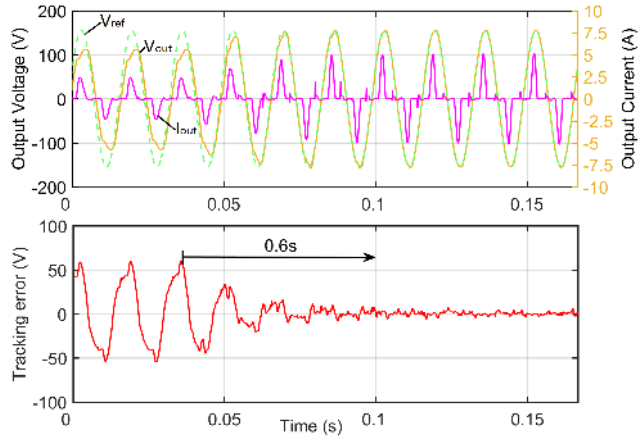

Fig. 11. Transient response of the traditional DFT-based selective harmonic RC under rectifier load under nominal reference frequency

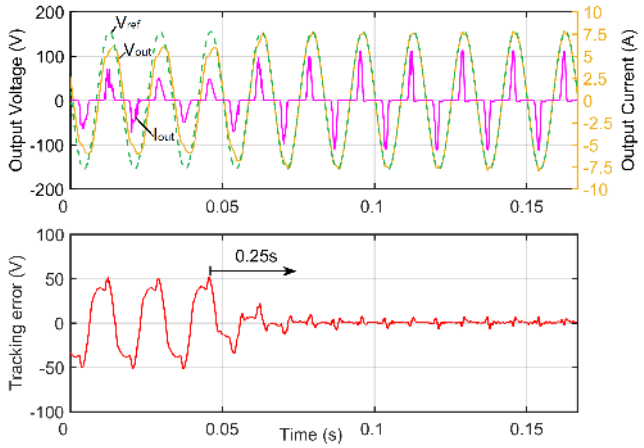

Fig. 12. Transient response of VVS DFT-based selective odd-order harmonic RC under rectifier load under nominal reference frequency

1) Transient response: Figs. 11 and 12 show the transient responses and tracking errors after applying the traditional DFT-based selective harmonic RC and VVS DFT-based selective odd-order harmonic RC with 60 Hz reference frequency under rectifier load, respectively. When the system operates under state feedback control, the peak tracking error is about 50 V due to the phase lag and magnitude error. After applying the DFT-based selective harmonic RC, the tracking error converges in 0.06 s. Because the proposed DFT-based selective odd-order harmonics RC is an only half reference period delay length compared with the traditional DFT-RC with one period delay, the transient speed gets about 50% improvement, which is shown as 0.025 s in Fig. 11.

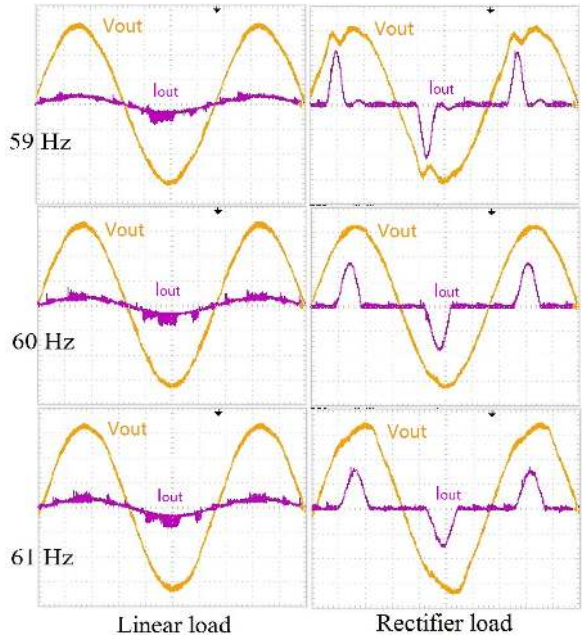

Fig. 13. Steady-state performance of the traditional DFT-based selective harmonic RC under linear load and rectifier load for 59 Hz, 60 Hz, and 61 Hz applications

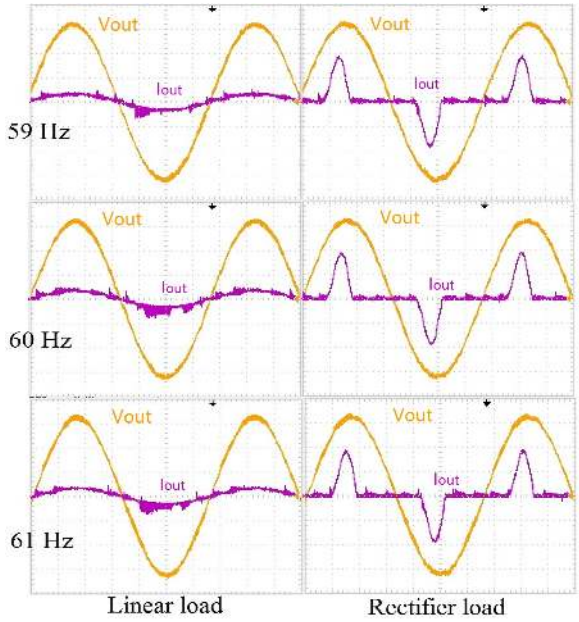

Fig. 14. Steady-state performance of VVS DFT-based odd-order harmonic RC under linear load and rectifier load for 59 Hz, 60 Hz, and 61 Hz applications

2) Steady-state performance: Figs. 13 and 14 show the steady-state performance of the DFT-based selective harmonic RC and VVS DFT-based selective odd-order harmonic RC under linear load and rectifier load for 59 Hz, 60 Hz, and 61 Hz applications. As shown in Fig. 13, the DFT-based selective harmonic RC is designed for 60 Hz application, so the steady-state outputs get severe distortion when the frequency is with

1 Hz fluctuation especially under rectifier load. Fig. 14 shows that, under VVS DFT-based selective odd-order harmonic RC, the steady-state outputs stay unchanged sinusoidal waveform under different kinds of loads when the frequency is under fluctuation. This is because the VVS is able to adaptively adjust the virtual sampling period according to varying signal period.

TABLE II
STEADY-STATE PERFORMANCE COMPARISON IN TERMS OF TRACKING ERROR AND THD FOR LINEAR LOAD (LL) AND RECTIFIER LOAD (RL)

		The DFT-based selective harmonic RC		VVS DFT-based selective odd-order harmonic RC	
		RMS error (V)	THD	RMS error (V)	THD
59 Hz	LL	4.69	1.49%	1.73	1.01%
	RL	8.86	7.16%	1.92	1.13%
60 Hz	LL	1.81	1.19%	1.64	1.12%
	RL	2.11	1.51%	1.93	0.92%
61 Hz	LL	3.16	1.27%	1.54	1.18%
	RL	8.56	5.53%	1.68	1.14%

The tracking accuracy of PWM inverters is normally evaluated in two important aspects: (1) THD concerning how sinusoidal the output is (in terms of power quality); (2) tracking error in root mean square (RMS) concerning the absolute control accuracy. Table II shows steady-state performance comparison for variable input frequency (59 Hz, 60 Hz, and 61 Hz) between the DFT-based selective harmonic RC and VVS DFT-based selective odd-order harmonic RC with linear load (LL) and rectifier load (RL). When reference input frequency deviates away from 60 Hz, the advantage of VVS DFT-based selective odd-order harmonic RC becomes significant. For 59 Hz and 61 Hz reference inputs, VVS DFT-based selective odd-order harmonic RC has lower tracking error (RMS errors are less than 2 V) and THD (THDs are about 1 %). For the traditional DFT-based selective harmonic RC, serious performance degradation occurs with 59 Hz and 61 Hz input signals. Compared with the traditional DFT-based selective harmonic RC, VVS DFT-based selective odd-order harmonic RC under LL shows 5% (59 Hz) and 84% (61 Hz) improvement in terms of THD and 39% (59 Hz) and 78% (61 Hz) improvement in terms of RMS tracking error. Similarly, VVS DFT-based selective odd-order harmonic RC under RL shows 29% (59 Hz) and 83% (61 Hz) improvement in terms of THD and 43% (59 Hz) and 77% (61 Hz) improvement in terms of RMS tracking error.

3) Load switch: Figs. 15 and 16 show the transient response of VVS DFT-based selective odd-order harmonic RC under sudden load switches from no load to linear load and from no load to rectifier load, respectively. The figures show that the output voltage recovers from sudden step load change in 1 cycle (0.017 s) when the linear load is switched on, and recovers within about 2 to 3 cycles (about 0.04 s) when rectifier load is switched on. This demonstrates that proposed VVS DFT-based selective odd-order harmonic RC is robust to load changes and has a quick transient response when the load changes.

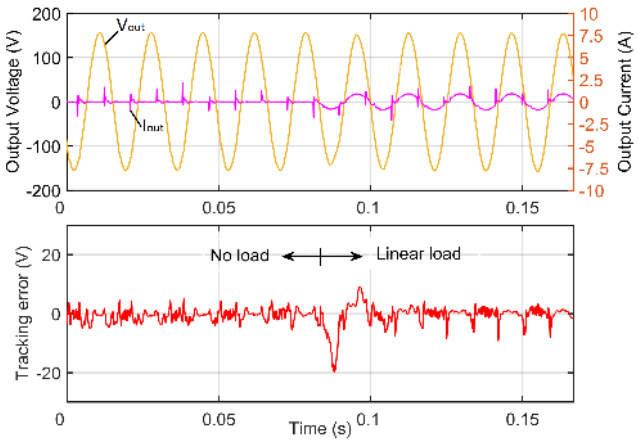

Fig. 15. Sudden load switch under VVS DFT-based selective odd-order harmonic RC from no load to linear load

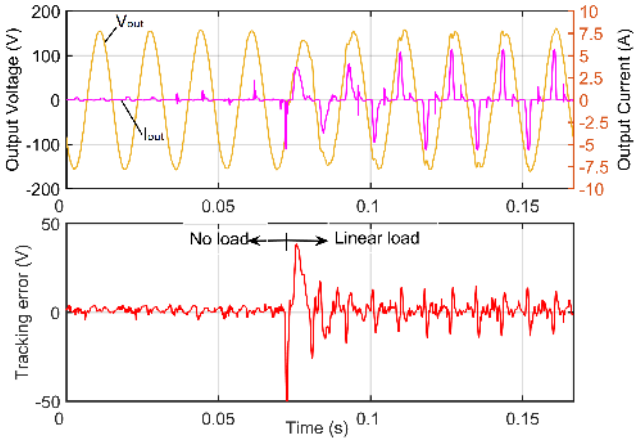

Fig. 16. Sudden load switch under VVS DFT-based selective odd-order harmonic RC from no load to rectifier load

4) Frequency fluctuation: Figs. 17 and 18 show the transient response comparison of the traditional DFT-based selective harmonic RC and VVS DFT-based selective odd-order harmonic RC when the reference frequency fluctuates. When the reference frequency changes from 60 Hz to 61 Hz, VVS DFT-based selective odd-order harmonic RC achieves very low tracking error and the peak-to-peak value about 10 V after a certain transient process. On the contrary, the peak-to-peak tracking error of the traditional DFT-based selective harmonic RC is about 30 V after the transient process. Therefore, the proposed VVS DFT-based selective odd-order harmonic RC shows obvious frequency adaptability with the reference frequency changing.

IV. CONCLUSION

In this paper, a simple, flexible, generic, and easy-to-implement virtual variable sampling method is proposed to address the performance degradation for variable frequency applications of the traditional DFT-based selective harmonic RC. With fixed system sampling period, a virtual variable sampling period is achieved by building an approximated virtual unit delay. Based on this, the DFT-based selective

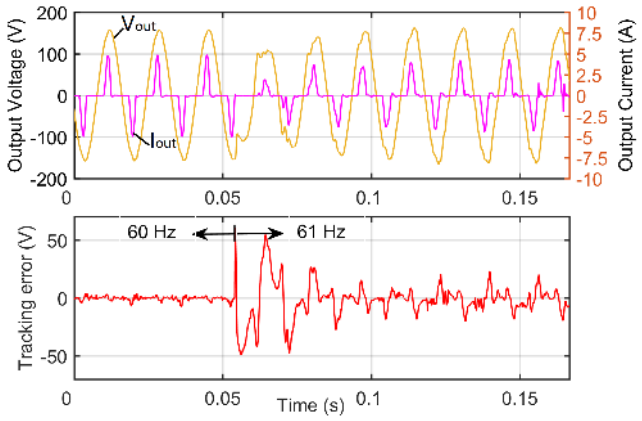

Fig. 17. Sudden frequency change of the traditional DFT-based selective harmonic RC under rectifier load

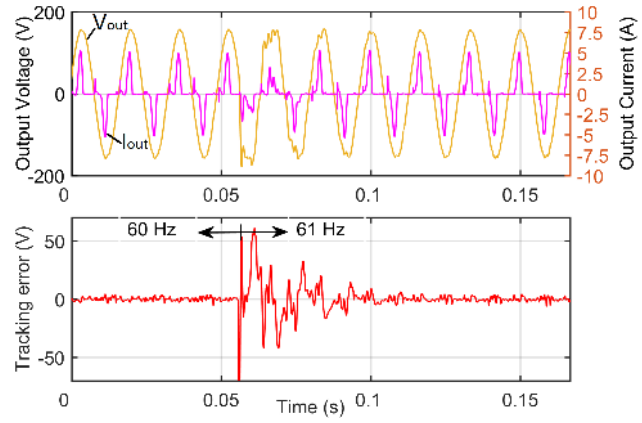

Fig. 18. Sudden frequency change of VVS DFT-based seletive odd-order harmonic RC under rectifier load

harmonic RC can be implemented with a virtual variable sampling period that is different from the system sampling period. Comparing with hardware-based variable sampling period methods, the proposed virtual variable sampling period is approximated by software and, therefore, is simpler and more cost-efficient. Moreover, a DFT-based selective odd-order harmonic RC is proposed, which has an only half number of delay elements comparing with the traditional DFT-based selective harmonic RC, and then leads to up 2 times faster transient response. Experimental results also show that VVS DFT-based selective odd-order harmonic RC offers better tracking performance and faster transient performance than the traditional DFT-based selective harmonic RC especially when the frequency is under fluctuation. The proposed virtual variable sampling also provides a flexible solution for other delay based controller design such as classic repetitive control [32].

APPENDIX

Proof of DFT filter performance:

For a particular harmonic h, the DFT filter without concerning phase lead N_a in Eq. (4) is:

$$\begin{aligned} F_{DFT}(z) &= \frac{4}{N}\sum_{i=0}^{N/2-1} cos\left(\frac{2\pi}{N}hi\right) z^{-i} \\ &= \frac{4}{N}\sum_{i=0}^{N/2-1} cos\left(\frac{2\pi}{N}hi\right) e^{-j\omega T_s i} \end{aligned} \tag{13}$$

where j is imaginary unit, ω is signal angular frequency and $\omega T_s = 2\pi k/N$ ($k \in \mathbb{N}$ is the input signal harmonic order).

$$\begin{aligned} &F_{DFT}(z) = \\ &\frac{4}{N}\sum_{i=0}^{N/2-1} cos\left(\frac{2\pi}{N}hi\right)\left[cos\left(\frac{2\pi}{N}ki\right) - j\cdot sin\left(\frac{2\pi}{N}ki\right)\right] \\ &= \frac{4}{N}\sum_{i=0}^{N/2-1}\left\{\frac{1}{2}\left[cos\left(\frac{2\pi}{N}(h+k)i\right) + cos\left(\frac{2\pi}{N}(h-k)i\right)\right]\right. \\ &\left. -\frac{1}{2}j\left[sin\left(\frac{2\pi}{N}(h+k)i\right) - sin\left(\frac{2\pi}{N}(h-k)i\right)\right]\right\} \end{aligned} \tag{14}$$

When h and k are both odd number, i.e. both $h+k$ and $h-k$ are even number, then

$$\sum_{i=0}^{N/2-1}\left[cos\left(\frac{2\pi}{N}(h+k)i\right)\right] = 0; \tag{15}$$

$$\sum_{i=0}^{N/2-1}\left[sin\left(\frac{2\pi}{N}(h+k)i\right)\right] = 0; \tag{16}$$

$$\sum_{i=0}^{N/2-1}\left[sin\left(\frac{2\pi}{N}(h-k)i\right)\right] = 0. \tag{17}$$

Thus, the DFT-based filter has unity magnitude and zero phase at the desired harmonics, $k = h$, and zero magnitude and zero phase at the other harmonics, $k \neq h$:

$$\begin{aligned} F_{DFT}(z) &= \frac{2}{N}\sum_{i=0}^{N/2-1} cos\left(\frac{2\pi}{N}(h-k)i\right) \\ &= \begin{cases} 1, & \text{when } k = h \\ 0, & \text{when } k \neq h \end{cases} \end{aligned} \tag{18}$$

REFERENCES

[1] Q. Zhao and Y. Ye, "Fractional phase lead compensation RC for an inverter: Analysis, design, and verification," *IEEE Transactions on Industrial Electronics*, vol. 64, no. 4, pp. 3127–3136, Apr 2017.

[2] S. H. Lee, W. J. Cha, B. H. Kwon, and M. Kim, "Discrete-time repetitive control of flyback CCM inverter for PV power applications," *IEEE Transactions on Industrial Electronics*, vol. 63, pp. 976–984, Feb 2016.

[3] R. Cardenas, M. Diaz, F. Rojas, J. Clare, and P. Wheeler, "Resonant control system for low-voltage ride-through in wind energy conversion systems," *IET Power Electronics*, vol. 9, no. 6, pp. 1297–1305, 2016.

[4] L. Jiang and D. Costinett, "A triple active bridge DC-DC converter capable of achieving full-range ZVS," in *2016 IEEE Applied Power Electronics Conference and Exposition*, Mar 2016, pp. 872–879.

[5] D. Pan, X. Ruan, C. Bao, W. Li, and X. Wang, "Optimized controller design for LCL-type grid-connected inverter to achieve high robustness against grid-impedance variation," *IEEE Transactions on Industrial Electronics*, vol. 62, no. 3, pp. 1537–1547, Mar 2015.

[6] S. Jiang, D. Cao, Y. Li, J. Liu, and F. Peng, "Low-THD, fast-transient, and cost-effective synchronous-frame repetitive controller for three-phase UPS inverters," *IEEE Transactions on Power Electronics*, vol. 27, no. 6, pp. 2994–3005, Jun 2012.

[7] Y. Wang, A. Darwish, D. Holliday, and B. W. Williams, "Plug-in repetitive control strategy for high-order wide-output range impedance-source converters," *IEEE Transactions on Power Electronics*, vol. 32, no. 8, pp. 6510–6522, Aug 2016.

[8] Z. Liu, B. Zhang, and K. Zhou, "Virtual delay unit based digital nk±m-order harmonic repetitive controller for PWM converter," in *Industrial Technology (ICIT), 2017 IEEE International Conference on*. IEEE, 2017, pp. 248–253.

[9] W. Rohouma, P. Zanchetta, P. Wheeler, and L. Empringham, "A four-leg matrix converter ground power unit with repetitive voltage control," *IEEE Transactions on Industrial Electronics*, vol. 62, pp. 2032–2040, Apr 2015.

[10] K. Zhou and D. Wang, "Digital repetitive controlled three-phase PWM rectifier," *Power Electronics, IEEE Transactions on*, vol. 18, no. 1, pp. 309–316, Jan 2003.

[11] B. Zhang, D. Wang, K. Zhou, and Y. Wang, "Linear phase lead compensation repetitive control of a CVCF PWM inverter," *Industrial Electronics, IEEE Transactions on*, vol. 55, no. 4, pp. 1595–1602, 2008.

[12] P. Mattavelli, "Synchronous-frame harmonic control for high-performance ac power supplies," *IEEE Transactions on Industry Applications*, vol. 37, no. 3, pp. 864–872, 2001.

[13] P. Mattavelli and F. P. Marafao, "Repetitive-based control for selective harmonic compensation in active power filters," *IEEE Transactions on Industrial Electronics*, vol. 51, no. 5, pp. 1018–1024, 2004.

[14] M. Herran, J. R. Fischer, S. Gonzalez, M. Judewicz, I. Carugati, and D. Carrica, "Repetitive control with adaptive sampling frequency for wind power generation systems," *IEEE Journal of Emerging and Selected Topics in Power Electronics*, vol. 2, pp. 58–69, Mar 2014.

[15] P. Zanchetta, M. Degano, J. Liu, and P. Mattavelli, "Iterative learning control with variable sampling frequency for current control of grid-connected converters in aircraft power systems," *IEEE Transactions on Industry Applications*, vol. 49, no. 4, pp. 1548–1555, Jul 2013.

[16] E. Kurniawan, Z. Cao, and Z. Man, "Design of robust repetitive control with time-varying sampling periods," *IEEE Transactions on Industrial Electronics*, vol. 61, no. 6, pp. 2834–2841, 2014.

[17] J. Olm, G. Ramos, and R. Costa-Castello, "Stability analysis of digital repetitive control systems under time-varying sampling period," *IET control theory & applications*, vol. 5, no. 1, pp. 29–37, 2011.

[18] T. Liu and D. Wang, "Parallel structure fractional repetitive control for PWM inverters," *IEEE Transactions on Industrial Electronics*, vol. 62, no. 8, pp. 5045–5054, Aug 2015.

[19] G. Escobar, M. Hernandez-Gomez, A. A. Valdez-Fernandez, M. J. Lopez-Sanchez, and G. A. Catzin-Contreras, "Implementation of a 6n ± 1 repetitive controller subject to fractional delays," *IEEE Transactions on Industrial Electronics*, vol. 62, no. 1, pp. 444–452, Jan 2015.

[20] Z. Zou, K. Zhou, Z. Wang, and M. Cheng, "Frequency-adaptive fractional-order repetitive control of shunt active power filters," *IEEE Transactions on Industrial Electronics*, vol. 62, pp. 1659–1668, Mar 2015.

[21] Y. Yang, K. Zhou, H. Wang, F. Blaabjerg, D. Wang, and B. Zhang, "Frequency adaptive selective harmonic control for grid-connected inverters," *IEEE Transactions on Power Electronics*, vol. 30, no. 7, pp. 3912–3924, Jul 2015.

[22] Z. Liu, B. Zhang, and K. Zhou, "Fractional-order phase lead compensation for multi-rate repetitive control on three-phase PWM DC/AC inverter," in *2016 IEEE Applied Power Electronics Conference and Exposition (APEC)*, Mar 2016, pp. 1155–1162.

[23] C. Xie, X. Zhao, M. Savaghebi, L. Meng, J. M. Guerrero, and J. C. Vasquez, "Multirate fractional-order repetitive control of shunt active power filter suitable for microgrid applications," *IEEE Journal of Emerging and Selected Topics in Power Electronics*, vol. 5, no. 2, pp. 809–819, 2017.

[24] Z. Liu, B. Zhang, and K. Zhou, "Universal fractional-order design of linear phase lead compensation multirate repetitive control for PWM inverters," *IEEE Transactions on Industrial Electronics*, 2017.

[25] D. Chen, J. Zhang, and Z. Qian, "An improved repetitive control scheme for grid-connected inverter with frequency-adaptive capability," *IEEE Transactions on Industrial Electronics*, vol. 60, pp. 814–823, Feb 2013.

[26] K. Zhou, D. Wang, B. Zhang, and Y. Wang, "Plug-in dual-mode-structure repetitive controller for CVCF PWM inverters," *IEEE Transactions on Industrial Electronics*, vol. 56, no. 3, pp. 784–791, 2009.

[27] R. Costa-Castelló, R. Grinó, and E. Fossas, "Odd-harmonic digital repetitive control of a single-phase current active filter," *IEEE Transactions on Power Electronics*, vol. 19, no. 4, pp. 1060–1068, 2004.

[28] B. Zhang, K. Zhou, and D. Wang, "Multirate repetitive control for PWM DC/AC converters," *IEEE Transactions on Industrial Electronics*, vol. 61, no. 6, pp. 2883–2890, Jun 2014.

[29] S. Yang, P. Wang, Y. Tang, and L. Zhang, "Explicit phase lead filter design in repetitive control for voltage harmonic mitigation of VSI-based islanded microgrids," *IEEE Transactions on Industrial Electronics*, vol. 64, no. 1, pp. 817–826, 2017.

[30] D. M. VandeSype, K. DeGusseme, F. M. DeBelie, A. P. VandenBossche, and J. A. Melkebeek, "Small-signal z-domain analysis of digitally controlled converters," *IEEE Transactions on Power Electronics*, vol. 21, no. 2, pp. 470–478, 2006.

[31] B. P. McGrath, S. G. Parker, and D. G. Holmes, "High-performance current regulation for low-pulse-ratio inverters," *IEEE Transactions on Industry Applications*, vol. 49, no. 1, pp. 149–158, 2013.

[32] K. Zhou, D. Wang, and K. Low, "Periodic errors elimination in CVCF PWM DC/AC converter systems: repetitive control approach," *IEE Proceedings-Control Theory and Applications*, vol. 147, pp. 694–700, 2000.

Zhichao Liu (S'16) received his B.E and M.E. degrees in electrical engineering from East China University of Science and Technology, China, in 2008 and 2011, respectively. He is currently working towards the Ph.D. degree in electrical engineering, University of South Carolina, Columbia, SC, USA.

From 2008 to 2011, he was with Shanghai Baosight software, Co., Ltd. Shanghai, China. His research interest includes advanced control theory and applications, digital control of power converter, and power electronics.

Bin Zhang (SM'08) received the B.E. and M.E. degrees from Nanjing University of Science and Technology, Nanjing, China, in 1993 and 1999, respectively, and the Ph.D. degree in Electrical Engineering from Nanyang Technological University, Singapore, in 2007.

Before he joined the Department of Electrical Engineering, University of South Carolina, Columbia, SC, USA, he was with General Motors R&D, Detroit, MI; Impact Technologies, Rochester, NY; and Georgia Institute of Technology, Atlanta, GA, USA. He has published over 100 technical papers. His current research interests include prognostics and health management, intelligent systems and controls, and their applications to various engineering systems.

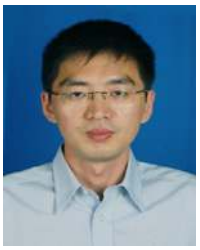

Keliang Zhou (M'04-SM'08) received the B.Sc. degree from the Huazhong University of Science and Technology, Wuhan, China, the M.Eng. degree from Wuhan Transportation University (now the Wuhan University of Technology), Wuhan, and the Ph.D. degree in Electrical Engineering from Nanyang Technological University, Singapore, in 1992, 1995, and 2002, respectively.

He is currently a Senior Lecturer with the School of Engineering at the University of Glasgow, Glasgow in U.K. since 2014. He has authored or coauthored one monograph on "Periodic Control of Power Electronic Converters", more than 100 technical papers and several granted patents in relevant areas. His teaching and research interests include power electronics and electric drives, renewable energy generation, control theory and applications, and microgrid technology.

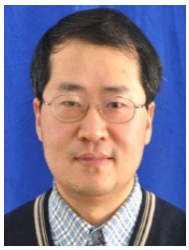

Jingcheng Wang received the B.S. and M.S. degrees from Northwestern Polytechnical University, Xian, China, in 1993 and 1995, respectively, and the Ph.D. degree from Zhejiang University, Hangzhou, China, in 1998.

He is currently a Professor with Shanghai Jiaotong University, Shanghai, China. His current research interests include robust control, intelligent control, real-time control, and simulation.